Driving Innovation ♦ Delivering Results

Electrocatalysis On a Nickel Complex at The Atomic Scale

D.N. Tafen,[1,2] D. Alfonso,[1] D. Kauffman,[1] and C. Matranga[1]

[1] Research & Innovation Center - NETL

[2] AECOM

Soda bubbles macro by en:User:Spiff via Wikimedia Commons. Microcapsules photo by by John Vericella/LLN

Motivation

General Approach For Electrochemical CO_2 Conversion

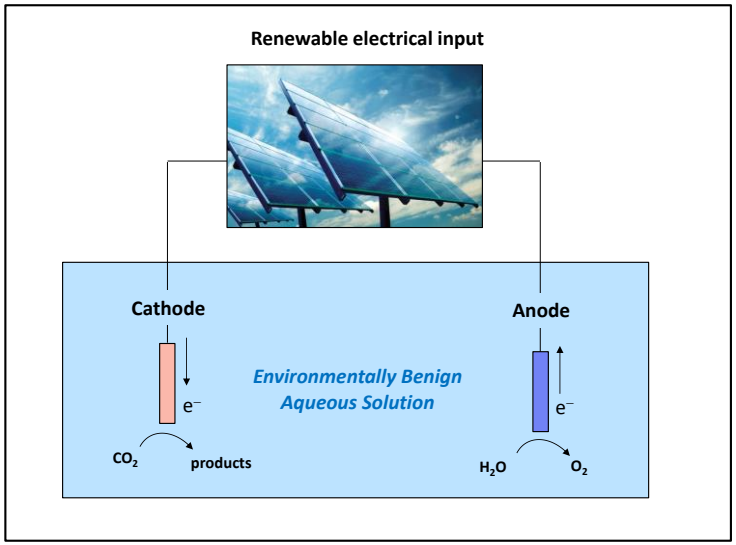

- **CO_2 is introduced into aqueous solution**
- **Electrons are injected from cathode catalyst into CO_2**
  - CO_2 + protons (H_2O) + electrons → products
- **Water is oxidized to O_2 at the anode (oxygen evolution reaction)**
  - Want to reduce overpotential and/or cost associated with Pt anode

The ability to computationally describe realistic working catalysts is important because it will facilitate the design of higher activity, earth-abundant catalysts by identifying accurate structure-property relationships.

*Smith et al. JACS **135**, 11580 (2013)*
*Yang et al. ACS Nano **8**, 9518 (2014)*
*Gao et al. JACS **136**, 7077 (2014)*

Computational Methods

- Implementation and Application of Multiscale Computational Infrastructure for Modeling Electrochemistry at Realistic Conditions

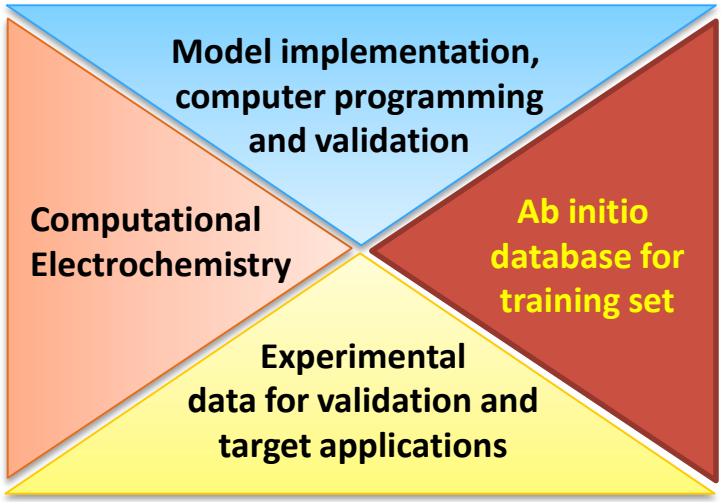

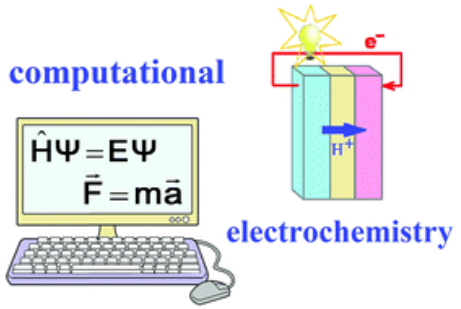

$H^+ + e^- \leftrightarrow \frac{1}{2} H_{2(g)}$ at STP, U = 0

$\mu(H^+ + e^-) = \frac{1}{2} \mu(H_2(g))$

- Reaction energy (Example, H_2O (l) + * $\leftrightarrow$ $OH_{ads} + H^+ + e^-$):

$$\Delta G = G_{OH^*} - G_{H_2O} - eU + kT \ln a_{H^+}$$

$$G = E + ZPE + TS$$

- Onset potential: $U_{onset} = \max((\Delta G_I, \Delta G_{II}, \Delta G_{III}, \ldots)/e)$

Bajdich et al. JACS, **135**, 13521 (2013)
Rossmeisl et al. J. Electroanal. Chem, **607**, 83 (2007)

OER Mechanism

- The OER mechanism is commonly described with four sequential one electron oxidation[1]

$$\text{(I)} \quad H_2O\,(l) + * \leftrightarrow OH_{ads} + H^+ + e^-$$

$$\text{(II)} \quad OH_{ads} \leftrightarrow O_{ads} + H^+ + e^-$$

$$\text{(III)} \quad O_{ads} + H_2O\,(l) \leftrightarrow OOH_{ads} + H^+ + e^-$$

$$\text{(IV)} \quad OOH_{ads} \leftrightarrow * + O_2\,(g) + H^+ + e^-$$

[1]Bajdich et al. JACS 2013, **135**, 13521
Kauffman, Alfonso, Tafen, et al. ACS Catalysis 2016, **6**, 1225

$Ni_6(PET)_{12}$ Structure and Characterization

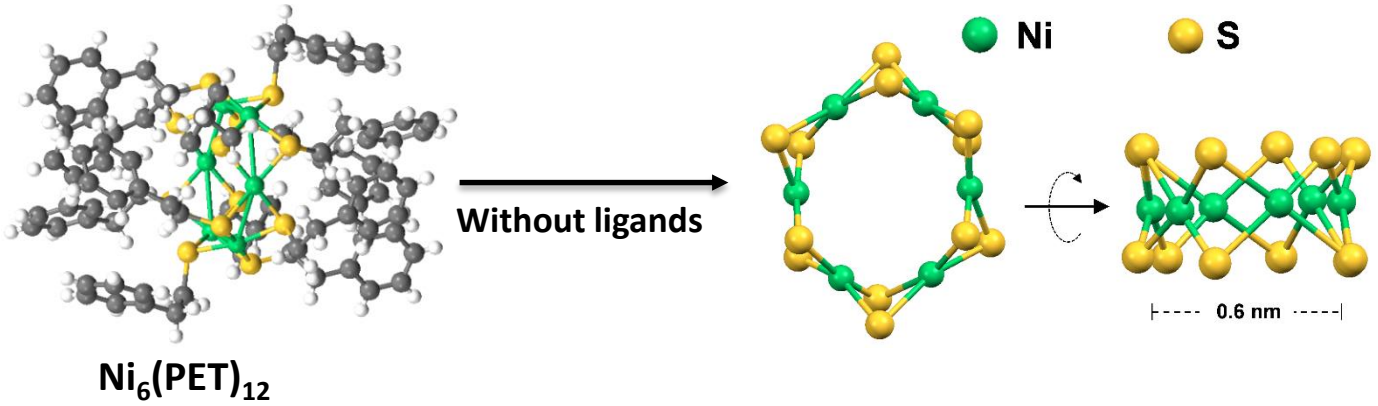

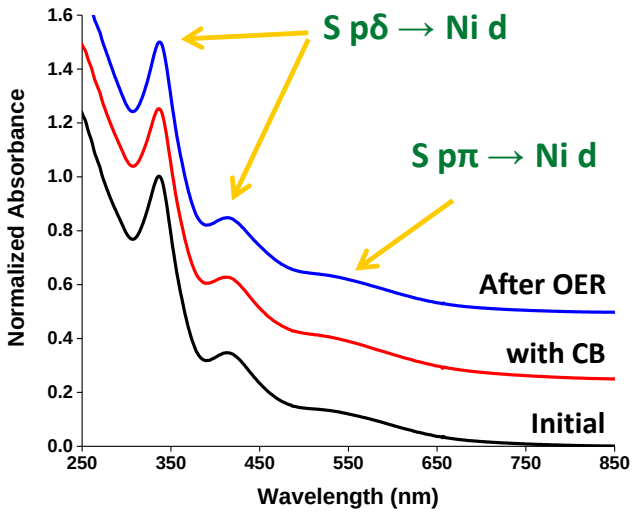

Optical absorbance spectra collected in dichloromethane

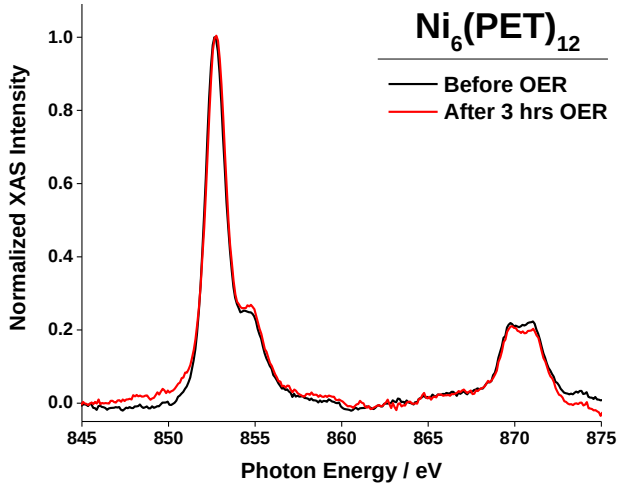

X-ray absorption spectra of $Ni_6(PET)_{12}$ before and after 3h OER electrolysis.

Electrocatalytic Data from Voltammetry and Steady State OER Electrolysis

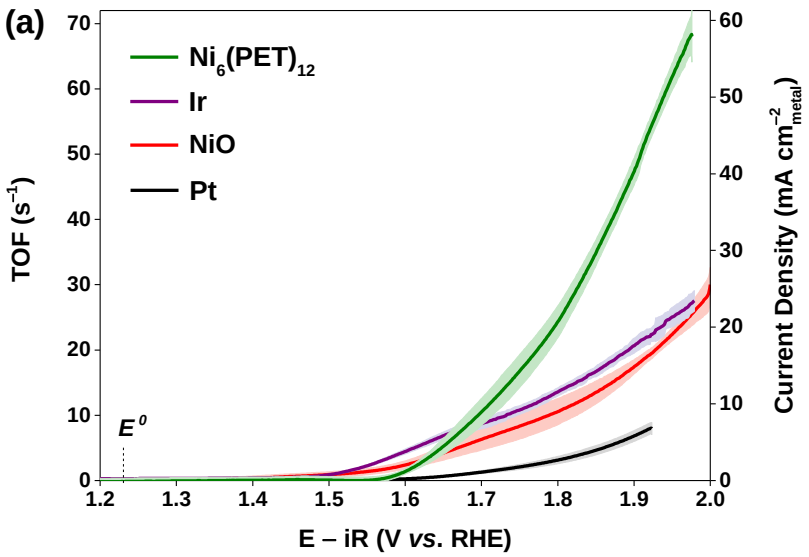

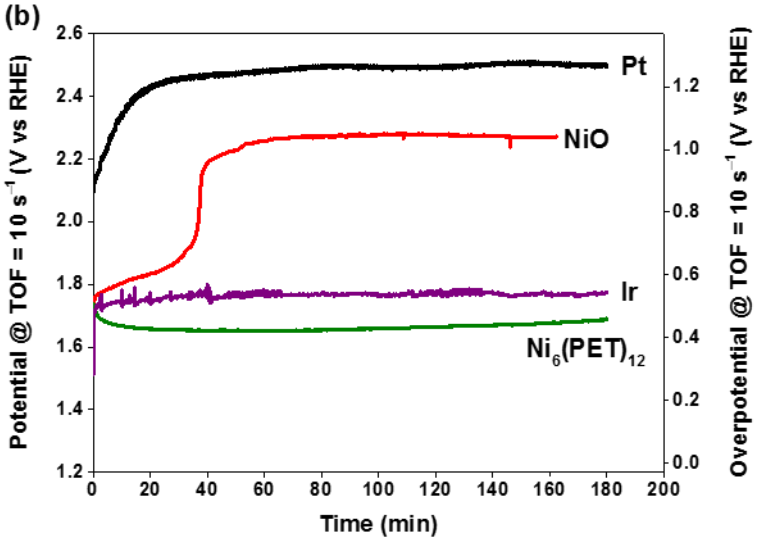

Material	OER Onset (V vs. RHE) [a]	Tafel Slope (mV dec^{-1}) [a]	η @ 10 s^{-1} (V vs. RHE) [a]	3 hour η @ 10 s^{-1} (V vs. RHE) [b]
$Ni_6(PET)_{12}$	1.544 ± 0.011	69 ± 12	1.700 ± 0.018	1.68
Ir	1.493 ± 0.009	54 ± 1	1.730 ± 0.019	1.77
NiO	1.575 ± 0.015	70 ± 5	1.812 ± 0.048	2.3
Pt	1.541 ± 0.009	60 ± 11	n/a[c]	2.5
CB	1.676 ± 0.006	255 ± 18	n/a[c]	n/a[c]

Table footnotes: η = overpotential; (a) from voltammetry data, (b) from electrolysis data, (c) did not occur within the considered iR-corrected potential window.

Stability Diagram of O-Covered $Ni_6(SCH_3)_{12}$

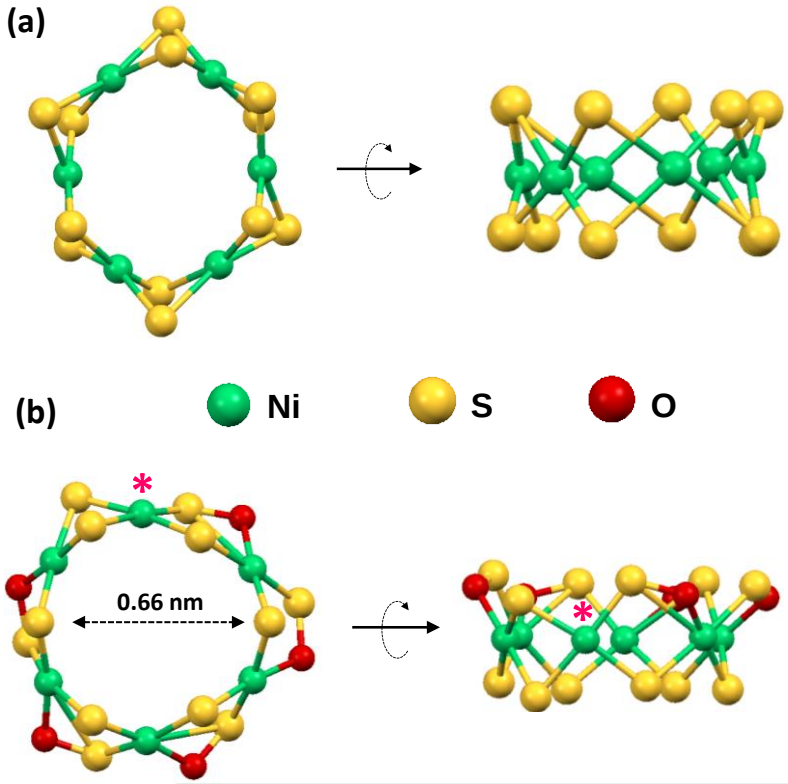

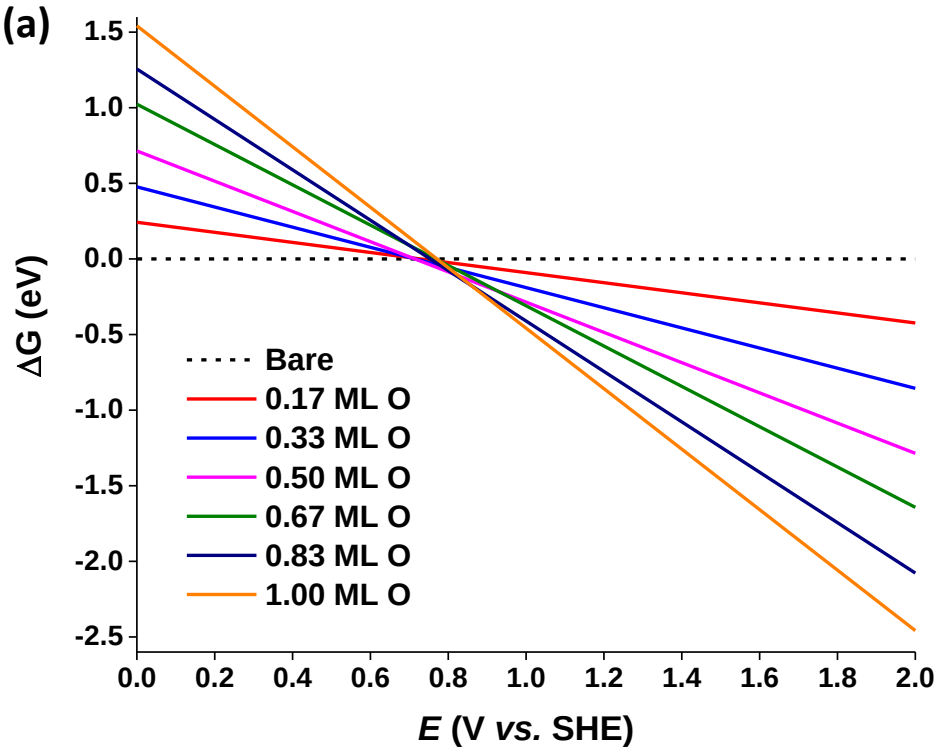

We considered the OER at Ni-S structure by including an implicit solvation model to describe the electrostatics, cavitation, and dispersion interactions between the solute and solvent.

Free Energy Diagram for OER at O-Covered $Ni_6(SCH_3)_{12}$

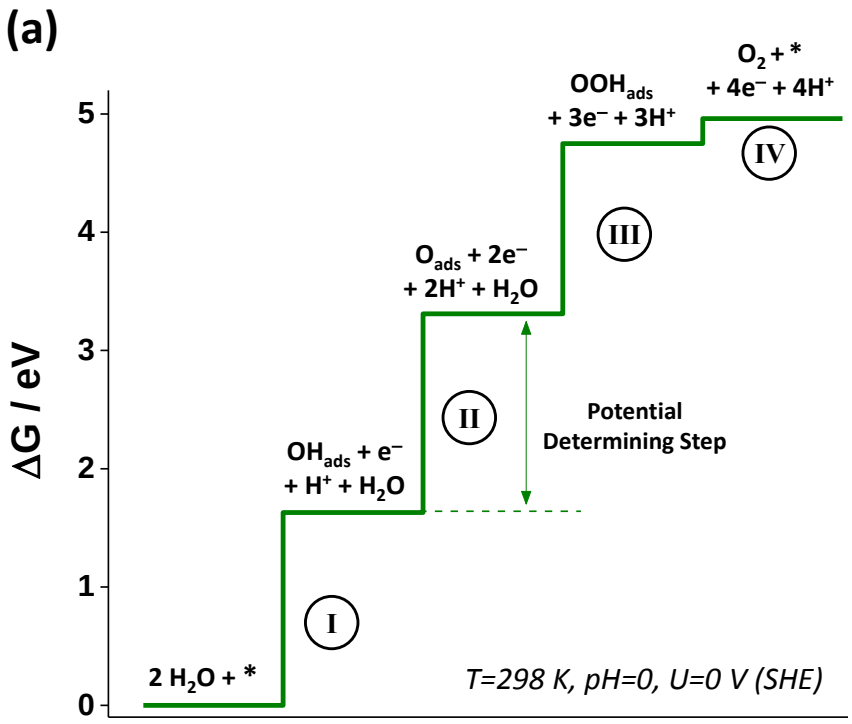

Step	Process	ΔG per step (eV)
Step I	H_2O (l) → OH_{ads}	1.63
Step II	OH_{ads} → O_{ads}	1.68
Step III	O_{ads} → OOH_{ads}	1.44
Step IV	OOH_{ads} → O_2 (g)	0.21
Total ΔG	$2H_2O$ (l) → O_2 (g)	4.96

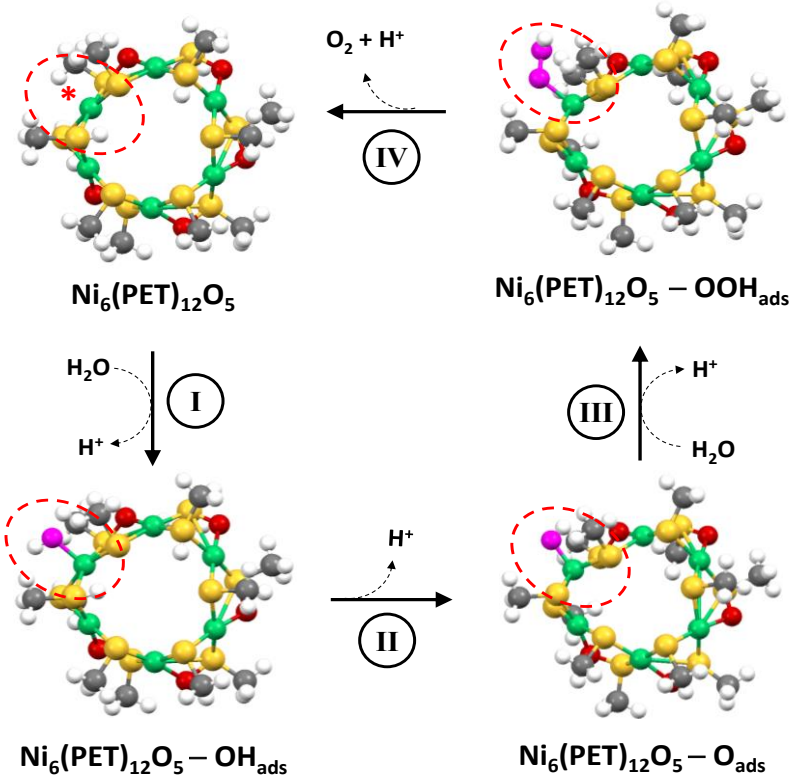

Theoretical potential E_{theo} = 1.24 V
OER formal potential E^0 = 1.23 V

PDS: 1-fold coordinated O_{ads}
Uonset = 1.68 V within ~0.14 V of our Expt

Comparison with Ir and Pt OER

Step	Process	ΔG (eV) $Ni_6(SCH_3)_{12}$	ΔG (eV) IrO_2 (110)	ΔG (eV) O-covered Pt(111)
I	H_2O (l) → OH_{ads}	1.63	0.45	1.43
II	OH_{ads} → O_{ads}	1.68	1.72	1.58
III	O_{ads} → OOH_{ads}	1.44	1.38	1.57
IV	OOH_{ads} → O_2 (g)	0.21	1.41	0.38
Total ΔG	$2H_2O$ (l) → O_2 (g)	4.96	4.96	4.96

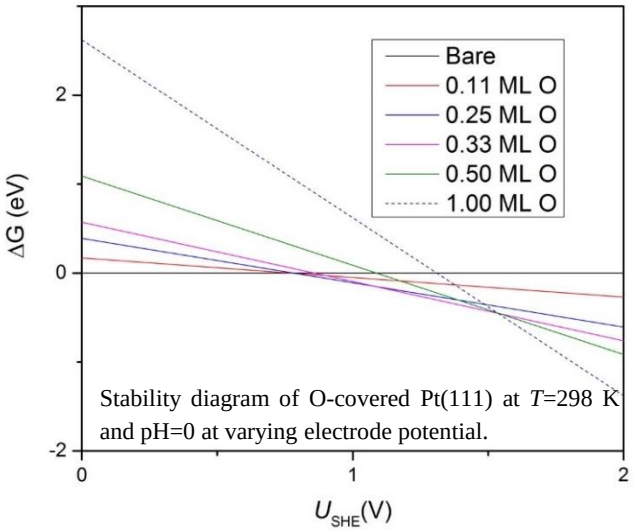

Stability diagram of O-covered Pt(111) at *T*=298 K and pH=0 at varying electrode potential.

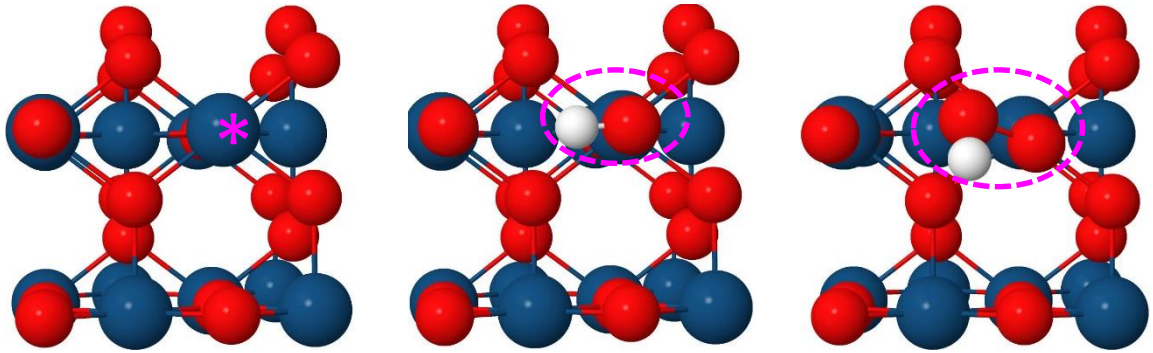

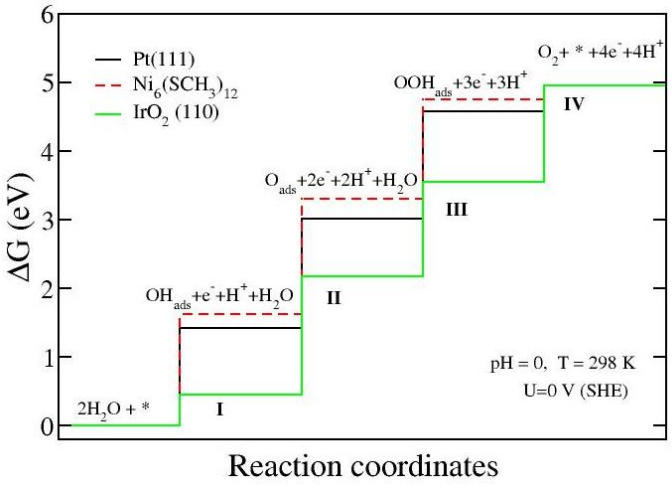

Influence of the Solvation Model

- Use an implicit solvation model as described by Hennig and coworkers
- Cavitation energies were evaluated employing a surface tension parameter of 0.525 meV/Å^2

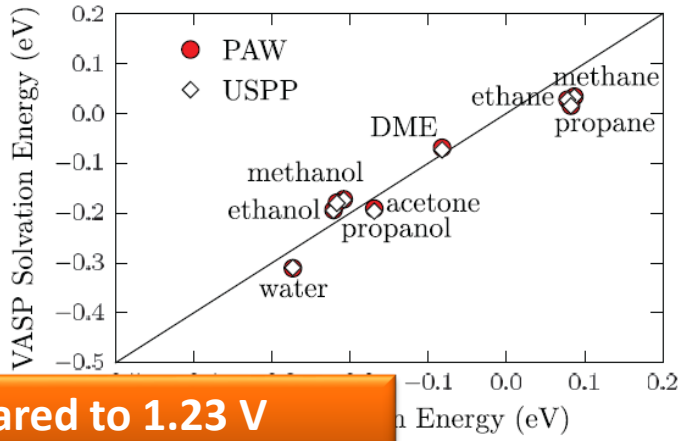

E_{theo} = 1.09 V compared to 1.23 V

	Process	Vacuum	Solvation
Step I	H_2O (l) → OH_{ads}	1.41	1.63
Step II	OH_{ads} → O_{ads}	1.74	1.68
Step III	O_{ads} → OOH_{ads}	1.13	1.44
Step IV	OOH_{ads} → O_2 (g)	0.08	0.21

Better agreement with Experiment

Matthew et al. J. Chem. Phys. **140**, 084106 (2014)

Summary and Conclusions

- We use a combination of experimental and computational techniques to study the OER at a supported organometallic nickel complex with a precisely known crystal structure.
- The $Ni_6(PET)_{12}$ complex out performed bulk NiO and Pt and showed OER activity comparable to Ir.
- Computational prediction of potential determining steps and OER onset potentials are in excellent agreement with experimentally determined values.
- The strategy used here allows atomic-level modeling of realistic catalyst structures and accurate descriptions of reaction mechanisms.
- Continued development of atomically-precise OER catalysts will help establish detailed structure activity relationships for the controlled synthesis of next generation OER catalysts.

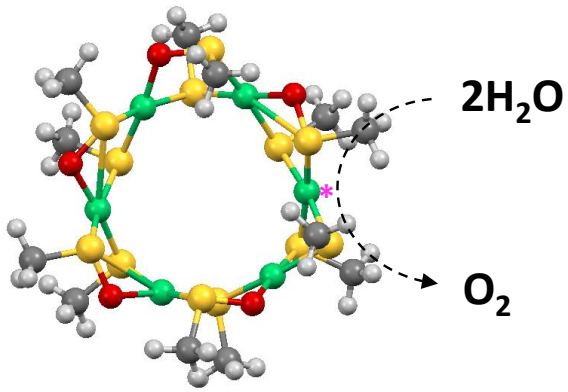

Acknowledgments

- Dominic R. Alfonso[1]
- Douglas R. Kauffman[1]
- Chris Matranga[1]
- Jonathan Lekse[1,2]
- Congjun Wang[1,2]
- Xingyi Deng[1,2]
- Junseok Lee[1,2]
- Santosh Kumar[1]
- Hoyoung Jang[3]
- Jun-sik Lee[3]

[1]Research & Innovation Center - MEM, National Energy Technology Lab
[2]AECOM
[3]Stanford Synchrotron Radiation Lightsource, SLAC National Accelerator Lab

Acknowledgments

- Portions of this work were performed in support of the National Energy Technology Laboratory's ongoing research under the RES contract DE-FE0004000. Use of the Stanford Synchrotron Radiation Lightsource (BL 8-2), SLAC National Accelerator Laboratory, is supported by the U.S. Department of Energy, Office of Science, Office of Basic Energy Sciences under Contract No. DE-AC02-76SF00515.

Disclaimers

- This report was prepared as an account of work sponsored by an agency of the United States Government. Neither the United States Government nor any agency thereof, nor any of their employees, nor AECOM, nor any of their employees, makes any warranty, express or implied, or assumes any legal liability or responsibility for the accuracy, completeness, or usefulness of any information, apparatus, product, or process disclosed, or represents that its use would not infringe privately owned rights.
- Reference herein to any specific commercial product, process, or service by trade name, trademark, manufacturer, or otherwise, does not necessarily constitute or imply its endorsement, recommendation, or favoring by the United States Government or any agency thereof. The views and opinions of authors expressed herein do not necessarily state or reflect those of the United States Government or any agency thereof.

It’s All About a Clean, Affordable Energy Future




For More Information, Contact NETL

the ENERGY lab

Delivering Yesterday and Preparing for Tomorrow